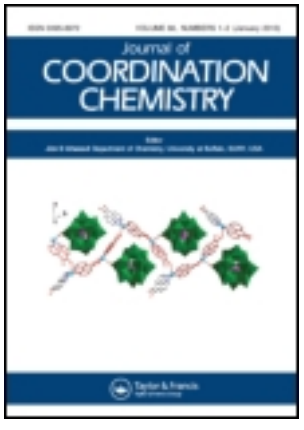

Journal of Coordination Chemistry
Publication details, including instructions for authors and subscription information:
http://www.tandfonline.com/loi/gcoo20

New dyes with enhanced two-photon absorption cross-sections based on the Cd(II) and 4′-(4-[4-(imidazole)styryl]phenyl)-2,2′:6′,2″-terpyridine

Dongling Xu [a], Mingdi Yang [a], Yang Wang [a], Yuanle Cao [a], Min Fang [a], Weiju Zhu [a], Hongping Zhou [a], Fuying Hao [a d], Jieying Wu [a] & Yupeng Tian [a b c]

[a] Department of Chemistry, Anhui University and Key Laboratory of Functional Inorganic Materials Chemistry of Anhui Province, Hefei, China

[b] State Key Laboratory of Crystal Materials, Shandong University, Jinan, China

[c] State Key Laboratory of Coordination Chemistry, Nanjing University, Nanjing, China

[d] Department of Chemistry, Fuyang Normal College, Fuyang, China

Accepted author version posted online: 28 Jun 2013.Published online: 30 Jul 2013.

To cite this article: Dongling Xu, Mingdi Yang, Yang Wang, Yuanle Cao, Min Fang, Weiju Zhu, Hongping Zhou, Fuying Hao, Jieying Wu & Yupeng Tian (2013) New dyes with enhanced two-photon absorption cross-sections based on the Cd(II) and 4′-(4-[4-(imidazole)styryl]phenyl)-2,2′:6′,2″-terpyridine, Journal of Coordination Chemistry, 66:17, 2992-3003, DOI: 10.1080/00958972.2013.819493

To link to this article: http://dx.doi.org/10.1080/00958972.2013.819493

Journal of Coordination Chemistry, 2013
Vol. 66, No. 17, 2992–3003, http://dx.doi.org/10.1080/00958972.2013.819493

New dyes with enhanced two-photon absorption cross-sections based on the Cd(II) and 4′-(4-[4-(imidazole) styryl]phenyl)-2,2′ : 6′,2″-terpyridine

DONGLING XU†, MINGDI YANG†, YANG WANG†, YUANLE CAO†, MIN FANG†, WEIJU ZHU†, HONGPING ZHOU*†, FUYING HAO†¶, JIEYING WU† and YUPENG TIAN†‡§

†Department of Chemistry, Anhui University and Key Laboratory of Functional Inorganic Materials Chemistry of Anhui Province, Hefei, China
‡State Key Laboratory of Crystal Materials, Shandong University, Jinan, China
§State Key Laboratory of Coordination Chemistry, Nanjing University, Nanjing, China
¶Department of Chemistry, Fuyang Normal College, Fuyang, China

(*Received 29 January 2013; in final form 5 June 2013*)

A series of new cadmium complexes (dyes **1**–**5**) were obtained by assembly of the donor–bridge–acceptor (D–π–A)-type ligand (L: 4′-(4-[4-(imidazole)styryl]phenyl) 2,2′ : 6′,2″-terpyridine) with CdX_2 (X=Cl, Br, I, NCS, ClO_4), in which dye **3** was characterized by single crystal X-ray diffraction. Various weak interactions, including hydrogen bonds (C–H···N, C–H···X) and π–π interactions, played significant roles in the final topological structures. Linear and non-linear optical properties of ligand and the complexes were investigated. The two-photon absorption cross-section of these complexes are larger than that of ligand with maximum values of 577 GM (dye **1**), 242 GM (dye **2**), 171 GM (dye **3**), 326 GM (dye **4**), and 215 GM (dye **5**) in N,N-dimethylformamide.

Keywords: Hydrogen bonds; π–π Interactions; Fluorescence; ICT; TPA

1. Introduction

Materials with intense two-photon absorption (TPA) have received attention as the most promising candidates for novel optical materials; their variety of potential applications includes three-dimensional microfabrication [1], information technology [2], laser technology [3], biological system imaging [4], etc. However, the bottleneck of application of TPA materials is the generally small TPA cross-sections (δ). TPA is a third-order non-linear optical (NLO) phenomenon, and the efficiency of this process is determined by measuring δ values, which urged us to synthesize materials with large TPA cross-sections. Several strategies were proposed to improve TPA response, such as taking both intramolecular and intermolecular approaches to enhance TPA efficiency [5], connecting donor and acceptor symmetrically or unsymmetrically by π-conjugated bridges to form D–π–D, A–π–A, or D–π–A structures and the building of multibranched molecules [6], which can

*Corresponding author. Email: zhpzhp@263.net

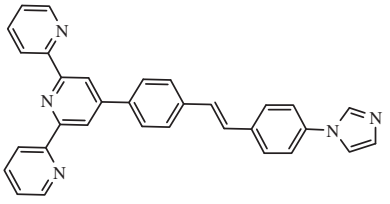

Figure 1. Schematic drawing of the ligand (**L**).

significantly enhance TPA cross-sections by increasing chromophore density of the molecules and the cooperative enhancement effect among the chromophores.

Coordination compounds are expected to show better physical and chemical stability, in which the metal ions serve either as a multidimensional template for increasing the density of two-photon active ligands [7] or as an important structural control in intramolecular charge transfer (ICT), leading to an enhanced δ value. Metal center can induce a strong intraligand charge-transfer transition, and the greater acceptor strength of metal center may boost δ values [8]. Also, a low-energy metal ligand charge-transfer transition may affect the δ value [9].

In this contribution, we used a reported D-π-A type ligand, 4′-(4-[4-(1H-1,2,4 triazolyl) styryl]phenyl)-2,2′ : 6′,2″-terpyridine (**L**) [10], to coordinate with CdX_2 (X=Cl, Br, I, NCS, ClO_4), in which the terpyridyl ring was the acceptor and an imidazolyl group acted as the donor (figure 1).

When the metal ion is bound to the acceptor, a new D-π-A structure is formed. The extended conjugated π-system should increase ICT upon excitation, which makes these complexes potential candidates for third-order NLO materials. Consequently, the organic and inorganic hybrid is expected to result in increased δ and enhanced fluorescence [11]. Our synthetic strategy is based on assembly of organic ligand with TPA properties and cadmium salts CdX_2 (X=Cl, Br, I, NCS, ClO_4) (scheme 1) and a series of new coordination complexes (dyes **1**–**5**) were produced, in which **3** was characterized by single crystal X-ray diffraction determination. Linear and NLO properties of the ligand and five dyes were investigated. The δ values of the five dyes were always larger than that of **L**, following the order, $Cl^- > SCN^- > Br^- > ClO_4^- > I^-$, which corresponded to our previous studies [12]. The halogen and halogenoid may affect the metal acceptance strength by different electron inductive effect.

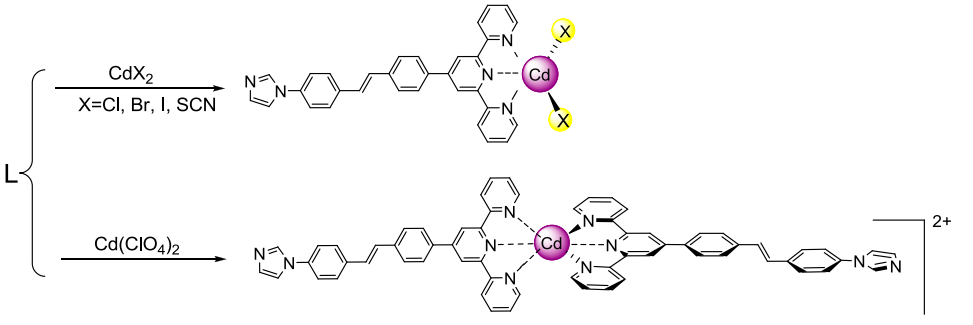

Scheme 1. Synthetic routes to dyes **1**–**5**.

2. Experimental

2.1. *Materials and physical measurements*

All chemicals were available commercially from Acros Organics Company (Beijing) and Aladdin (Shanghai), and the solvents were purified via conventional methods before use. UV–vis absorption spectra were recorded on a UV-3100 spectrophotometer. Fluorescence measurements were carried out using an Edinburgh FLS920 fluorescence spectrometer equipped with a 450 W Xe lamp and a time-correlated single-photon counting card. All solvents used in the test were chromatographically pure reagents. The two-photon excited fluorescence (TPEF) spectra were measured using a mira 900-D Ti : sapphire femtosecond laser with a pulse width of 200 fs and a repetition rate of 76 MHz. IR spectra were recorded with a Nicolet FT-IR NEXUS 870 spectrometer (KBr disks) from 4000 to 400 cm^{-1}. TPA cross-sections were measured using fluorescein as reference. Elemental analyses were measured by a Perkin Elmer 240B elemental analyzer.

2.2. *Preparation of ligand and dyes 1–5*

Ligand: ***L*** has been synthesized according to the reference procedure [10].

*$CdLI_2{\cdot}CHCl_3$ (dye **3**)*: CdI_2 (18.31 mg, 0.05 mM) in 15 mL of MeOH was layered onto a solution of **L** (23.85 mg, 0.05 mM) in 5 mL of $CHCl_3$ and after several days gave yellow acicular single crystals. Yield: 32 mg (76%). FT-IR (KBr, cm^{-1}): 3441 (m), 1595 (vs), 1570 (m), 1521 (s), 1474 (s), 1424 (m), 1400 (m), 1301 (m), 1246 (m), 1052 (m), 1012 (m), 963 (m), 835 (m), 789 (m), 747 (m). Anal. Calcd for $C_{32}H_{23}I_2N_5Cd$: C, 45.55; H, 2.75; N, 8.30%. Found: C, 45.45; H, 2.77; N, 8.27%.

By the same method, we obtained the other four dyes:

*$CdLCl_2$ (dye **1**)*: FT-IR (KBr, cm^{-1}): 3441 (m), 1597 (vs), 1571 (m), 1521 (s), 1475 (s), 1426 (m), 1402 (m), 1304 (m), 1248 (m), 1057 (m), 1014 (m), 963 (m), 837 (m), 791 (m), 731 (m). Anal. Calcd for $C_{32}H_{23}Cl_2N_5Cd$: C, 58.16; H, 3.51; N, 10.60%. Found: C, 58.25; H, 3.47; N, 10.49%.

*$CdLBr_2$ (dye **2**)*: FT-IR (KBr, cm^{-1}): 3441 (m), 1596 (vs), 1571 (m), 1520 (s), 1474 (s), 1428 (m), 1401 (m), 1305 (m), 1248 (m), 1060 (m), 1014 (m), 963 (m), 836 (m), 791 (m), 730 (m). Anal. Calcd for $C_{32}H_{23}Br_2N_5Cd$: C, 51.26; H, 3.09; N, 9.34%. Found: C, 51.15; H, 3.07; N, 9.39%.

*$CdL(NCS)_2$ (dye **4**)*: FT-IR (KBr, cm^{-1}): 3438 (m), 3124 (w), 2054 (vs), 1598 (vs), 1571 (m), 1520 (vs), 1475 (s), 1424 (m), 1401 (m), 1303 (m), 1245 (m), 1162 (m), 1113 (m), 1063 (m), 1012 (m), 963 (m), 834 (m), 790 (m), 731 (m). Anal. Calcd for $C_{34}H_{23}N_7S_2Cd$: C, 57.83; H, 3.28; N, 13.89%. Found: C, 57.66; H, 3.26; N, 13.86%.

*$CdL_2(ClO_4)_2$ (dye **5**)*: FT-IR (KBr, cm^{-1}): 3437 (m), 1599 (vs), 1572 (m), 1522 (s), 1476 (s), 1426 (m), 1403 (m), 1305 (m), 1249 (m), 1093 (vs), 1015 (s), 965 (m), 838 (m), 793 (m), 747 (m), 621 (m). Anal. Calcd for $C_{64}H_{46}Cl_2N_{10}O_8Cd$: C, 60.70; H, 3.66; N, 11.06%. Found: C, 60.53; H, 3.64; N, 11.12%.

2.3. *X-ray crystallography*

X-ray diffraction data of single crystals were collected on a Siemens Smart 1000 CCD diffractometer. Determination of unit cell parameters and data collections were performed

with Mo Kα radiation ($\lambda = 0.71073$ Å). Unit cell dimensions were obtained with least-squares refinements, and all structures were solved by direct methods using *SHELXS-97* [13]. The other nonhydrogen atoms were located in successive difference Fourier syntheses. The final refinement was performed using full-matrix least-squares with anisotropic thermal parameters for nonhydrogen atoms on F^2. Hydrogens were added theoretically, riding on the concerned atoms.

3. Results and discussion

3.1. *Structure of dye 3*

Crystallographic data and processing parameters for dye **3** are shown in table 1. Selected bond lengths and angles for dye **3** are listed in table 2. Dye **3** crystallizes in the monoclinic form with space group *C2/c*, as shown in table 1. Figure 2(a) shows the coordination environment of Cd[II] with atom numbering scheme. The unit consists of a cadmium ion connecting with three N of **L** and two iodides, and a free chloroform molecule. The bond lengths of Cd1–N1, Cd1–N2, and Cd1–N3 are 2.345(4), 2.331(4), and 2.385(4) Å, respectively. Bond angles around the cadmium are 68.8(1) to 135.9(9)°, which indicate quite distorted trigonal bipyramid geometry. Selected bond lengths and angles are listed in table 2.

There is a chloroform connected with the ligand via C–H···Cl bond interactions (rose dashed line, d (H25···Cl1) = 2.559 Å and the angle of C25–H25···Cl1 is 143.977°) (figure 2(a)). As shown in figure 2(b), chloroform plays a vital role in the structure as bridges (d (H25···Cl1) = 2.559 Å, d (H13···Cl3) = 2.711 Å (sky blue dashed line), and angle of C25–H25···Cl1 is 143.977°). The imidazole ring is not directly involved in coordination, but the lone pair electrons from N have a strong electron-donating ability, which provides the condition for forming a 1-D chain along the *b*-axis. From figure 2(c),

Table 1. Crystallographic data for dye **3**.

Compound	$CdLI_2{\cdot}CHCl_3$ (dye **3**)
Empirical formula	$C_{33}H_{24}Cl_3I_2N_5Cd$
Formula weight	963.12
Crystal system	Monoclinic
Space group	*C2/c*
a [Å]	21.430(5)
b [Å]	17.583(5)
c [Å]	17.844(5)
β [°]	91.728(5)
V [Å^3]	6721(3)
Z	8
T [K]	298(2)
D_{Calcd} [g cm^{-3}]	1.904
μ [mm^{-1}]	2.758
θ range [°]	1.50–25.00
Total no. data	5921
No. unique data	4876
No. parameters refined	397
R_1	0.0401
wR_2	0.1387
GOF	1.181

Table 2. Selected bond lengths (Å) and angles (°) for dye **3**.

$CdLI_2 \cdot CHCl_3$ (dye **3**)			
Cd1–N1	2.345(4)	I1–Cd1–I2	114.379(20)
Cd1–N2	2.331(4)	I1–Cd1–N1	106.9(9)
Cd1–N3	2.385(4)	I1–Cd1–N2	109.401(94)
Cd1–I1	2.752(8)	I1–Cd1–N3	98.871(115)
Cd1–I2	2.736(8)	I2–Cd1–N1	102.588(89)
N1–Cd1–N2	68.807(126)	I2–Cd1–N2	135.868(92)
N1–Cd1–N3	135.476(129)	I2–Cd1–N3	98.810(114)

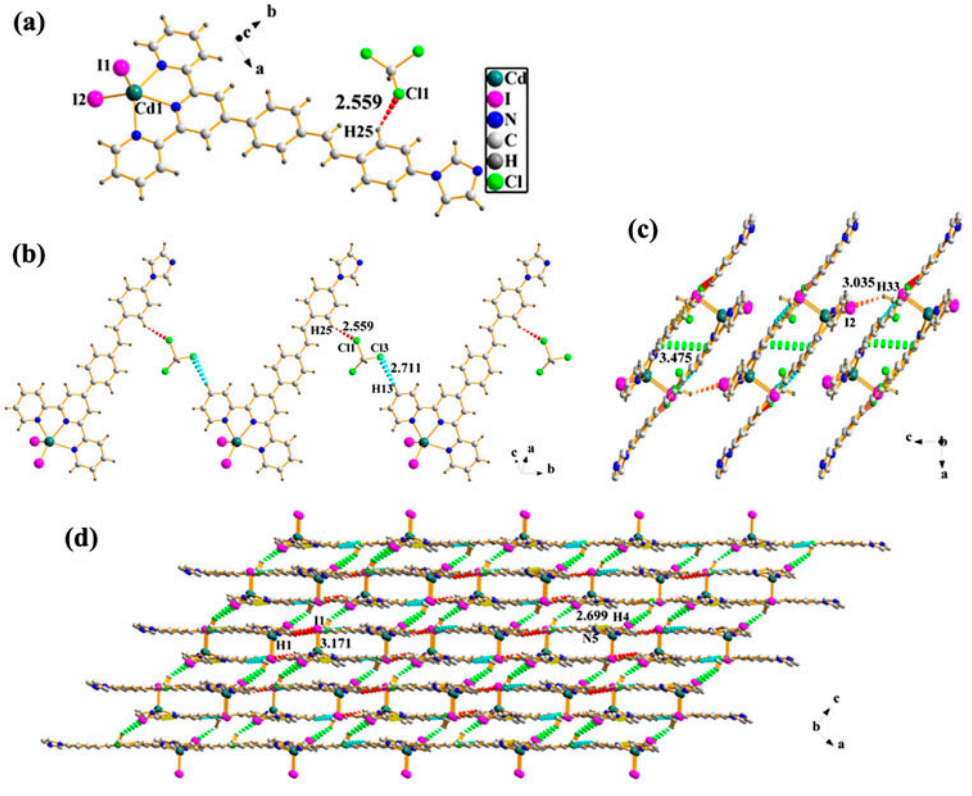

Figure 2. (a) Coordination environment of Cd with atom numbering scheme. (b) The 1-D chain of dye **3** showing the C–H···N (rose and blue) hydrogen bond along the *b*-axis. (c) The 2-D layered framework of dye **3** showing C–H···I hydrogen bond and π–π stacking along the *c*-axis. (d) The 3-D architecture of dye **3** showing the C–H···I and C–H···N hydrogen bonds (red and yellow) along the *a*-axis (see http://dx.doi.org/10.1080/00958972.2013.819493 for color version).

dye **3** formed a 2-D framework through π–π stacking interactions (green dashed line, the shortest distance is 3.475 Å, plum dashed line, the shortest distance is 3.035 Å) between the neighboring dimers along the *c*-axis. In addition, C–H···I interactions (d (H33···I2) = 3.035 Å, the angle of C33–H33···I2 is 141.207°) play a significant role. Finally, extended 3-D topological structures are formed along the *a*-axis *via* C–H···I and C–H···N interactions (red dashed line, d (H1···I1) = 3.171 Å, d (H4···N5) = 2.699 Å), the angle of C1–H1···I1 is 102.198° and the angle of C4–H4···N5 is 155.703° (figure 2(d)).

The unit cell of dye **3** contains one $CdLI_2$. From the element analyses and coordination structures of similar ligands and salts in the literature [14], we infer the unit cells of dyes **1**, **2**, and **4** may contain one $CdLX_2$; the unit cell of dye **5** contains one $CdL_2\ (ClO_4)_2$.

3.2. *Linear absorption and single-photon excited fluorescence (SPEF)*

The photophysical properties (absorption and fluorescence) of the new series of dyes in five different solvents are collected in table 3, including fluorescence quantum yields.

3.2.1. Absorption properties. Linear absorption properties of **L** and **1**–**5** in tetrahydrofuran (THF), ethyl acetate, ethanol, acetonitrile, and N,N-dimethylformamide (DMF) ($1.0 \times 10^{-5}\,M\,L^{-1}$) were studied. Each of their absorption spectra exhibits two absorption bands centered at 279–290 and 325–348 nm (figure 3). The low energy band (325–348 nm) is assigned to ICT transition [14a]. The high energy band (279–290 nm) is the characteristic peak of terpyridyl [15], which is assigned to π–π^* transitions [16]. The absorption profile and maxima of all of the compounds are almost identical in different solvents, suggesting that ground state electronic structures are independent of solvent polarity and small dipole moments associated with the ICT transitions.

Table 3. Photophysical properties of dyes **1**–**5** in five different polar solvents.

Compound	Solvents	$\lambda_{max}^{(1a)a}$	$\lambda_{max}^{(1f)b}$	Φ^c	$\Delta\nu^d$
Dye **1**	THF	287, 333	416	0.601	5992
	Ethyl acetate	287, 341	466	0.288	7866
	Ethanol	290, 345	461	0.185	7294
	Acetonitrile	286, 340	514	0.157	9957
	DMF	281, 332	433	0.488	7026
Dye **2**	THF	282, 335	418	0.559	5927
	Ethyl acetate	287, 341	467	0.336	7912
	Ethanol	290, 340	461	0.204	7720
	Acetonitrile	287, 340	514	0.147	9957
	DMF	281, 331	433	0.471	7117
Dye **3**	THF	282, 335	414	0.503	5696
	Ethyl acetate	283, 338	411	0.377	5255
	Ethanol	289, 340	459	0.232	7625
	Acetonitrile	286, 340	514	0.129	9957
	DMF	281, 332	434	0.521	7079
Dye **4**	THF	282, 334	415	0.808	5844
	Ethyl acetate	287, 340	409	0.283	4962
	Ethanol	288, 341	462	0.276	7680
	Acetonitrile	286, 339	513	0.099	10,005
	DMF	281, 333	433	0.478	6935
Dye **5**	THF	283, 333	414	0.541	5875
	Ethyl acetate	285, 338	411	0.341	5255
	Ethanol	290, 343	462	0.195	7509
	Acetonitrile	287, 338	432, 509	0.178	9939
	DMF	281, 331	433	0.550	7117

[a]Peak position of the longest absorption band.
[b]Peak position of SPEF, excited at the absorption maximum.
[c]Quantum yields determined by using quinine sulfate as standard.
[d]Stokes shift in cm^{-1}.

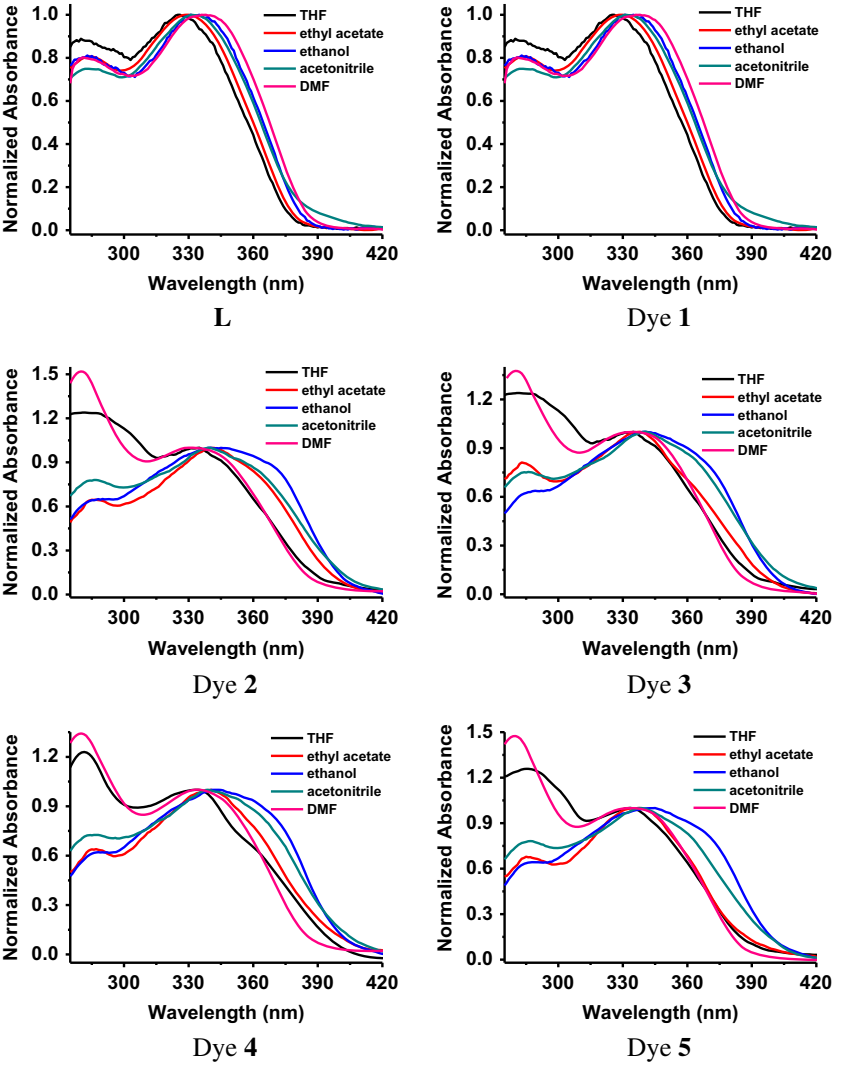

Figure 3. Linear absorption spectra of **L** and **1**–**5** in solvent with different polarity.

3.2.2. Fluorescence properties. The SPEF quantum yields (Φ) were measured by using a standard method under the same experimental conditions for all compounds. The data step is 1 nm, 400 mV excitation voltage, and excitation slit width and emission slit widths were 5.0 nm. Quinine sulfate dissolved in 0.1 M L^{-1} sulfuric acid (Φ = 0.577) [17] was used as the standard. The SPEF spectra were measured at the same concentration as that of the linear absorption spectra. The absorption spectrum is not sensitive to solvent polarity, however, with increasing solvent polarity, the emission wavelengths shift dramatically except in DMF. As shown in figure 4, the SPEF spectra of **L** and **1**–**5** display pronounced positive solvatochromism (i.e. bathochromic shift with increasing solvent polarity) in their emission spectra. The emission maxima of **L** and **1**–**5** are about 415 nm

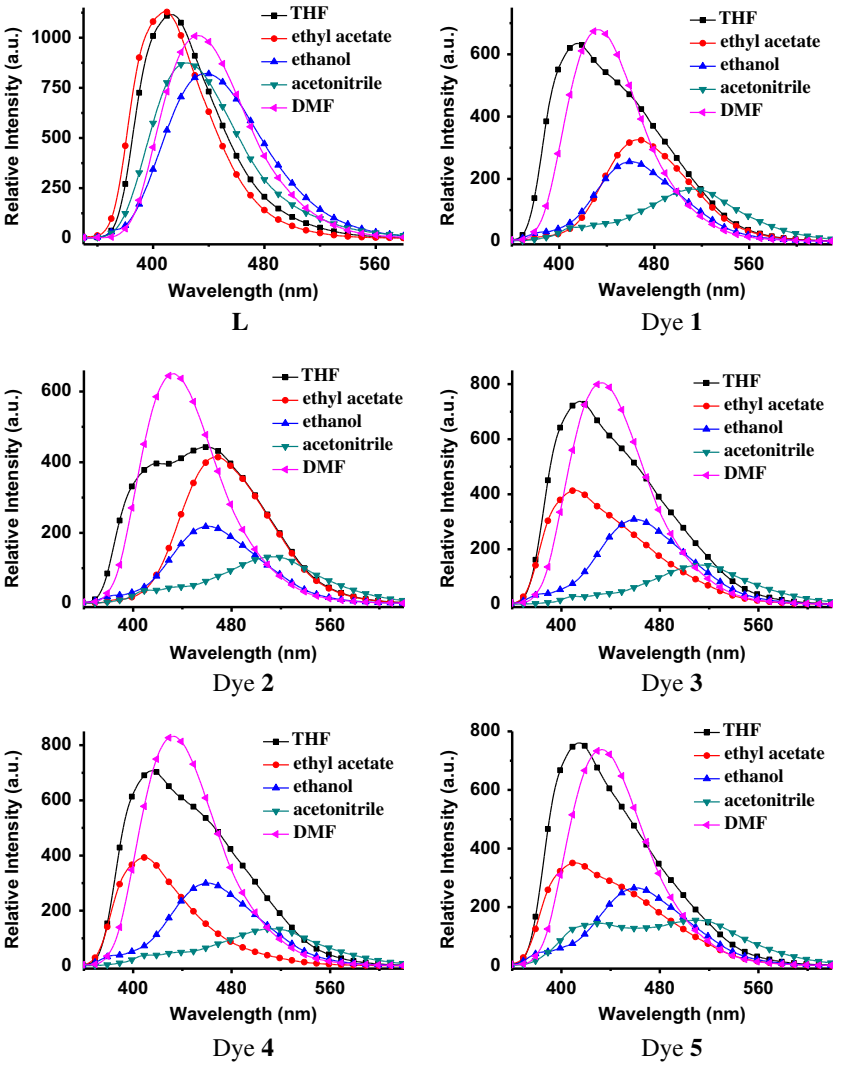

Figure 4. The one-photon fluorescence spectra of **L** and **1**–**5**.

in THF. In polar acetonitrile, the peak is located at 514 nm, red-shifted by 100 nm due to the different molecular environment. Large Stokes shifts are observed for **L** and **1**–**5** in five solvents due to strong solvent–solute dipole–dipole interactions, a manifestation of the large dipole moment and orientational polarizability. Because **L** and **1**–**5** contain an electron-donating group and an electron-withdrawing group, they exhibit a significant dipole moment in the ground state, which depends on charge separation in the fluorophore. In the excited state, it is likely that this charge separation increases, which results in a larger dipole moment than that in the ground state [18]. Such an increase in dipole moment would explain the sensitivity of the emission spectra of these dipolar compounds to solvent polarity. As solvent polarity increases, the fluorescence quantum yields show a decreasing trend.

3.3. *Two-photon excited fluorescence*

There is no linear absorption in the wavelength range 450–850 nm for the ligand and the complexes, which indicates that there are no molecular energy levels corresponding to an electron transition in the spectral range. Therefore, upon excitation from 450 to 850 nm, it is impossible to produce single-photon-excited up-converted fluorescence. If frequency up-converted fluorescence induced with a laser in this spectral range appears, it can be ascribed to TPEF. Figure 5 shows a log–log plot of the excited fluorescence signal *versus* excited light power, providing direct evidence for squared dependence of excited fluorescence power and input laser intensity.

As shown in figure 6, the TPA spectra of **L** and **1**–**5** are determined in the wavelength range by investigating their TPEF in DMF with a concentration of $1.0 \times 10^{-3}\,\mathrm{M\,L^{-1}}$. Absorption maxima are at 443 and 488 nm for **L** and 538 nm for **1**–**5** in DMF. Similar to SPEF spectra, the TPEF peak positions do not depend on excitation wavelengths. Nevertheless, the intensity of two-photon fluorescence has relationship with excitation wavelengths. Figure 6 shows that the two-photon fluorescence intensity has significant dependence on the excitation wavelengths; for dyes **1**–**5**, the best excitation wavelengths are 740, 740, 740, 730, and 760 nm, respectively.

The TPA cross-sections (δ) are determined by comparing their TPEF to that of fluorescein in DMF, according to the following equation [19]:

$$\delta = \delta_{\mathrm{ref}} \frac{\Phi_{\mathrm{ref}}}{\Phi} \frac{c_{\mathrm{ref}}}{c} \frac{n_{\mathrm{ref}}}{n} \frac{F}{F_{\mathrm{ref}}}$$

The subscripts ref stand for the reference molecule, δ is the TPA cross-section value, c is the concentration of solution, n is the refractive index of the solution, F is the TPEF integral intensities of the solution emitted at the excitation wavelength, and Φ is the fluorescence quantum yield. The δ_{ref} was taken from the literature [20].

Detailed experiments reveal that from 715 to 830 nm the peak position in TPEF spectra of these complexes is independent of the excitation wavelength, but the TPA cross-sections are dependent over this range. By tuning the pump wavelength incrementally from 715 to 830 nm while keeping the input power fixed and then recording the TPEF intensity, the TPA spectra are obtained. By referencing the TPA cross-section of fluorescein to be 38 GM ($1\mathrm{GM} = 10^{-50}\,\mathrm{cm^{-4}\,s\,photon^{-1}}$) [21], the maximum TPA cross sections of

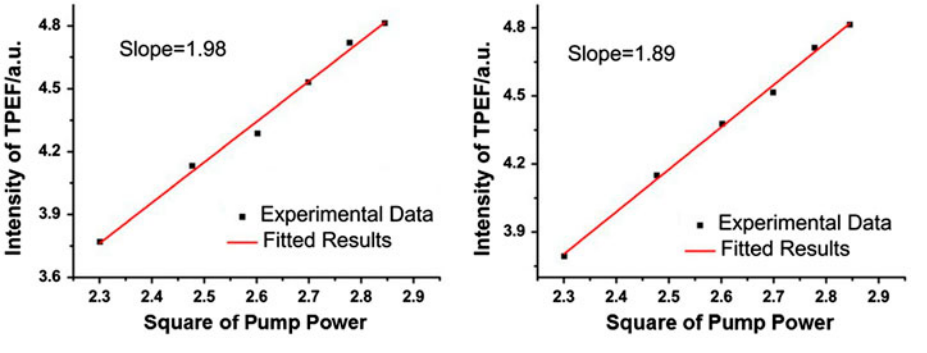

Figure 5. Output fluorescence intensity (I_{out}) *vs.* the square of input laser power $(I_{\mathrm{in}})^2$ for **L** (left) and **1** (right) in DMF. Excitation carried out at 720 nm, with $c = 1.0 \times 10^{-3}\,\mathrm{M\,L^{-1}}$ in DMF.

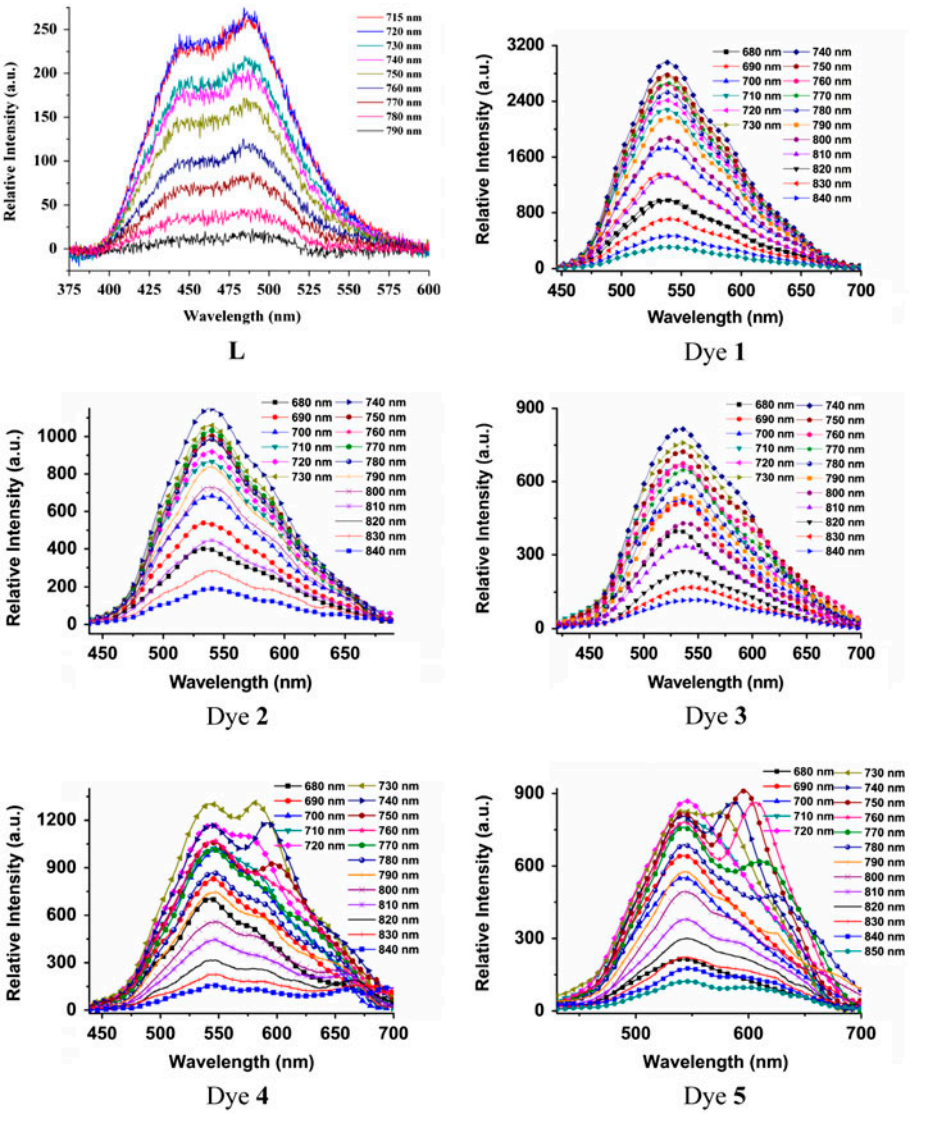

Figure 6. The TPA spectra of **L** and **1**–**5** in DMF under different excitation wavelengths ($c = 1.0 \times 10^{-3}$ M L^{-1}).

complexes are 149 for **L** (720 nm), and 577 (720 nm), 242 (740 nm), 171 (740 nm), 326 (730 nm) and 215 GM (720 nm), for **1**–**5**, respectively, in DMF.

Figure 7 shows the TPA spectrum of **L** and **L**–Cd (II) from 715 to 830 nm. TPA cross-sections of **L**-Cd (II) from 715 to 830 nm are always larger than that of **L**, which is unusual for Cd complexes. The behavior observed here in the TPA spectra can be attributed to enlarged conjugation length upon Cd(II) bonded to **L**, a new D-π-A type compound, in which the terpyridyl ring is the acceptor and an imidazolyl is the donor. Presumably Cd(II) withdraws electron density from the terpyridyl, increasing the overall conjugation length. When **L** is coordinated with Cd(II), a stronger acceptor is formed,

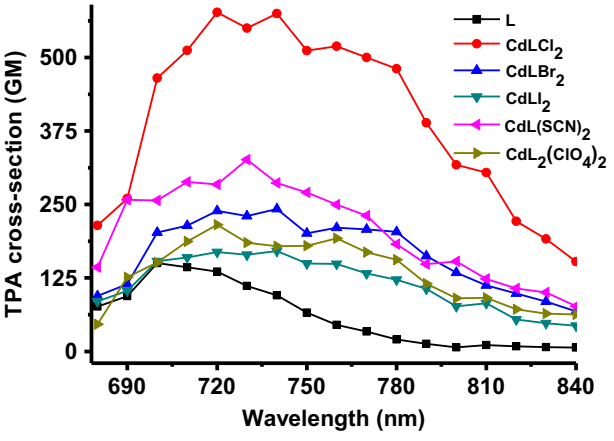

Figure 7. Two-photon (from a 200 fs, 76 MHz, Ti : sapphire laser) absorption cross-sections of **L** and **1**–**5** in DMF versus excitation wavelengths of identical energy of 0.100 w (experimental uncertainties: 10%).

which induces a larger localization of the electrons. So the TPA cross-sections of the Cd(II) complexes increase compared to that of free ligand.

4. Conclusions

A series of new coordination complexes (dyes **1**–**5**) are synthesized by self-assembly of 4′-(4-[4-(imidazolyl)styryl]phenyl)-2,2′ : 6′,2″-terpyridine with CdX_2 (X=Cl, Br, I, SCN, ClO_4). Solvent and various weak interactions, including hydrogen bonds (C–H···N, C–H···X) and π–π contacts, play significant roles in the final topological structures. TPA-induced fluorescence of the dyes at 715–830 nm increased obviously after **L** coordinated with CdX_2, ascribed to enlarged conjugation length when Cd(II) becomes the acceptor. Considering polymeric cadmium complexes containing 8-hydroxyquinoline were used as dye sensitizers for dye-sensitized solar cells [22], we will prepare compounds with broad spectral coverage and excellent charge separation and transportation by introducing groups such as –OH, –COOH, and assembly with cadmium salts, which expand the use of the material.

Supplementary material

Crystallographic data reported in this contribution has been deposited with the Cambridge Crystallographic Data Center, CCDC No. 835527 for dye **3**. Copies of this information may be obtained free of charge from the Director, CCDC, 12 Union Road, Cambridge CB2 1EZ, UK (Fax: +44-1223/336-033; E-mail: deposit@ccdc.cam.ac.uk).

Acknowledgements

This work was supported by Program for New Century Excellent Talents in University (China), Doctoral Program Foundation of Ministry of Education of China (20113401110004), National Natural Science Foundation of China (21271003, 21271004), Natural Science Foundation of Education Committee of Anhui Province (KJ2012A024,

KJ2013B205), the 211 Project of Anhui University, the Anhui University Students Innovative Entrepreneurial Training Program (cxcy2012035), the Anhui University Students Research Training Program, the Team for Scientific Innovation Foundation of Anhui Province (2006KJ007TD), and Ministry of Education Funded Projects Focus on Returned Overseas Scholar.

References

[1] (a) S. Kawata, H.-B. Sun, T. Tanaka, K. Takada. *Nature*, **412**, 697 (2001); (b) W. Zhou, S.-M. Kuebler, K.-L. Braun, C.-K. Ober, J.-W. Perry, S.-R. Marder. *Science*, **296**, 1106 (2002).
[2] S. Kawata, Y. Kawata. *Chem. Rev.*, **100**, 1777 (2000).
[3] C. Ye, J. Wang, D. Lo. *Appl. Phys. B*, **78**, 539 (2004).
[4] K.-A. Kasischke, H.-D. Vishwasrao, P.-J. Fisher, W.-R. Zipfel, W.-W. Webb. *Science*, **305**, 99 (2004).
[5] (a) E. Collini. *Phys. Chem. Chem. Phys.*, **14**, 3725 (2012); (b) J. Yoo, S.-K. Yang, M.-Y. Jeong, H.-C. Ahn, S.-J. Jeon, B.-R. Cho. *Org. Lett.*, **5**, 645 (2003); (c) M. Albota, D. Beljonne, J.-L. Brédas, J.-E. Ehrlich, J.-Y. Fu, C. Xu. *Science*, **281**, 1650 (1998).
[6] A. Abbotto, L. Beverina, R. Bozio, G.-A. Pagani, D. Pedron, R. Signorini. *Chem. Commun.*, **17**, 2144 (2003).
[7] J.-P. Sauvage. *Acc. Chem. Res.*, **23**, 319 (1990).
[8] X.-J. Liu, J.-K. Feng, A.-M. Ren, H. Cheng, X. Zhou. *J. Chem. Phys.*, **120**, 11493 (2004).
[9] (a) L.-K. Chen, G.-B. Shaw, I. Novozhilova, T. Liu, G.-J. Meyer, P. Coppens. *J. Am. Chem. Soc.*, **125**, 7022 (2003); (b) M.-P. Cifuentes, C.-E. Powell, J.-P. Morrall, N.-T. Lucas, M.-G. Humphrey, S. Houbrechts. *J. Am. Chem. Soc.*, **128**, 10819 (2006).
[10] H.-P. Zhou, F.-X. Zhou, P. Wu, Z. Zheng, Z.-P. Yu, Y.-X. Chen, Y.-L. Tu, L. Kong, J.-Y. Wu, Y.-P. Tian. *Dyes Pigm.*, **91**, 237 (2011).
[11] S. Sumalekshmy, M.-M. Henary, K. Schmidt, J. Brédas, J.-W. Perry, C.-J. Fahrni. *J. Am. Chem. Soc.*, **129**, 11888 (2007).
[12] (a) H.-P. Zhou, J.-Q. Wang, F.-X. Zhou, D.-L. Xu, Y.-L. Cao, G. Liu. *Dyes Pigm.*, **95**, 723 (2012); (b) F.-X. Zhou, Z. Zheng, H.-P. Zhou, W.-Z. Ke, J.-Q. Wang, Z.-P. Yu, F. Jin, J.-X. Yang, Y.-Y. Wu, Y.-P. Tian. *CrystEngComm*, **14**, 5613 (2012).
[13] O. Mongin, L. Porres, C. Kahn, T. Pons, J. Mertz, D.-M. Blanchard. *Tetrahedron Lett.*, **44**, 8121 (2003).
[14] S. Ershad, L. Saghatrfroush, J. Khodmarz, S.-G. Telfer. *Int. J. Electrochem. Sci.*, **6**, 3997 (2011).
[15] D.-M. Li, Q. Zhang, P. Wang, J.-Y. Wu, J.-X. Yang, H.-P. Zhou. *Dalton Trans.*, 8170 (2011).
[16] B.-A. Maynard, P.-A. Smith, L.-A. Ladner, A. Jaleel, N.-E. Sykora, N. Beedoe, C. Crawford, Z. Assefa. *Inorg. Chem.*, **48**, 6425 (2009).
[17] G.-A. Reynolds, K.-H. Drexhage. *Opt. Commun.*, **13**, 222 (1975).
[18] Y.-H. Gao, J.-Y. Wu, H.-P. Zhou, J.-X. Yang, S.-Y. Zhang, Y.-P. Tian. *J. Am. Chem. Soc.*, **131**, 5208 (2009).
[19] C. Xu, W.-W. Webb. *J. Org. Chem. B*, **13**, 481 (1997).
[20] O. Varnavski, T. Goodson, L. Sukhomlinova, R. Twieg. *J. Phys. Chem. B*, **108**, 10484 (2004).
[21] M.-A. Albota, C. Xu, W.-W. Webb. *Appl. Opt.*, **37**, 7352 (1998).
[22] L.-R. Zhang, G.-J. Wen, Q. Xiu, L.-H. Guo, J.-Y. Deng, C.-F. Zhong. *J. Coord. Chem.*, **65**, 1632 (2012).